

Comparison of Quantum Yield of Upconversion Nanocrystals Determined by Absolute and Relative Methods

Eduard Madirov, Dmitry Busko, Fernando Arteaga Cardona, Damien Hudry, Sergey V. Kuznetsov, Vasilii A. Konyushkin, Andrey N. Nakladov, Alexander A. Alexandrov, Ian A. Howard, Bryce S. Richards,* and Andrey Turshatov*

Photoluminescence quantum yield (ϕ) is a key parameter of any luminescent material. There are two main ways to determine this value: 1) absolute, which requires calculation of the number of emitted and absorbed photons; and 2) relative, which utilizes the emission of a reference sample with known ϕ . Both methods become more complicated in case of upconversion (UC) photoluminescence, due to its nonlinear nature. The main obstacle to employing the relative method is the lack of a suitable reference with known UC quantum yield (UCQY, ϕ_{UC}). Herein, a new UCQY reference material is presented, based on SrF₂:1%Yb³⁺,1%Er³⁺ single crystal, for the relative measurement of ϕ_{UC} for near-infrared (976 nm)-to-visible UC. When utilizing this reference material, the ϕ_{UC} is determined to be 2.5% (at 100 W cm⁻²) for α -NaYF₄:18%Yb³⁺,2%Er³⁺@CaF₂ nanocrystals (NCs). This result coincides very well with the value for the same NCs determined using the absolute method of $\phi_{UC} = 2.4%$ (at 100 W cm⁻²). The intensity dependence of UCQY yield for the NCs determined using the SrF₂:1%Yb³⁺,1%Er³⁺ reference exhibits good agreement with the results acquired with the absolute method. In addition, various effects that can have an impact on the measured UCQY using absolute and relative methods are discussed.

1. Introduction

Upconversion (UC) is a process resulting in emission of one photon with higher energy after absorption of two or more photons with lower energy. Particularly, UC materials based on lanthanides ions attract interest due to their relevance for many optical applications, including nanoprobe for bioimaging,^[1] solar radiation converters,^[2,3] optical thermometers,^[4] and inks used for security purposes.^[5] As new UC materials are being developed in many laboratories worldwide, figures-of-merit describing their photoluminescence (PL) performance are required to compare UC materials in a useful manner. A commonly used parameter for characterization of photoluminescent materials—the emission quantum yield (ϕ)—is defined as the ratio of the number of photons emitted to the number of photons absorbed. It must be noted that the UC quantum yield


(UCQY, ϕ_{UC}), also commonly used for UC materials, is not a constant but varies with excitation intensity due to the nonlinear nature of the UC mechanism. Therefore, the excitation intensity (excitation power per area) must be controlled in the measurement and quoted in the presentations of the results. The parameter defined above and used throughout this text is the internal quantum yield, that is, the number of emitted photons divided by the number of absorbed photons. For applications wherein the brightness of the emission of the sample under given excitation conditions is most important, the slightly different external quantum yield is used, which is the number of emitted photons divided by the number of incident photons. This external quantum efficiency is equal to the internal quantum efficiency multiplied by the fraction of incident photons that are absorbed.

The ϕ values of PL materials are usually measured using one of two methods:^[6–8] 1) the absolute method, where the number of absorbed and emitted photons is estimated using various techniques such as an integrating sphere,^[9] photoacoustics,^[10] actinometry,^[11] or calorimetry^[12]; and 2) the relative method, where the PL of a sample is compared to the PL of a reference. The use of an integrating sphere—along with a laser and a

E. Madirov, D. Busko, F. A. Cardona, D. Hudry, I. A. Howard, B. S. Richards, A. Turshatov
Institute of Microstructure Technology
Karlsruhe Institute of Technology
Hermann-von-Helmholtz-Platz 1, 76344 Eggenstein-Leopoldshafen, Germany
E-mail: bryce.richards@kit.edu; andrey.turshatov@kit.edu

S. V. Kuznetsov, V. A. Konyushkin, A. N. Nakladov, A. A. Alexandrov
Research Center of Laser Materials and Technology
Prokhorov General Physics Institute of the Russian Academy of Sciences
Vavilov Str, 38, 119991 Moscow, Russia

I. A. Howard, B. S. Richards
Light Technology Institute
Karlsruhe Institute of Technology
Engesserstrasse 13, 76131 Karlsruhe, Germany

 The ORCID identification number(s) for the author(s) of this article can be found under <https://doi.org/10.1002/adpr.202200187>.

© 2022 The Authors. Advanced Photonics Research published by Wiley-VCH GmbH. This is an open access article under the terms of the Creative Commons Attribution License, which permits use, distribution and reproduction in any medium, provided the original work is properly cited.

DOI: 10.1002/adpr.202200187

spectrofluorometer—is the most commonly implemented method to determine the absolute UCQY, defined as $\phi_{UC}^{(a)}$.^[13–19] It should be emphasized that there is a key difference between measurements of the quantum yield for materials having a Stokes-shifted PL and UC (anti-Stokes) PL: that is that ϕ_{UC} demonstrates a dependence on the excitation intensity. At low excitation intensities ϕ_{UC} behaves as $\phi_{UC} = I^{n-1}$, where I is the excitation intensity ($W\ cm^{-2}$) and n is the number of photons involved in the UC process whereas (ideally) at higher excitation intensities it saturates and ϕ_{UC} approaches a constant value. In practice, the observed ϕ_{UC} can reach a maximum at a given I and then decrease as heating or higher order channels reduce the efficiency of the population of the emitting state. Thus, it is essential to report ϕ_{UC} in combination with the precise excitation intensity used in the experiment. Even better is to report the intensity dependence of ϕ_{UC} over a broad intensity range—usually in the range 10^{-1} – $10^2\ W\ cm^{-2}$. A series of past publications have confirmed that $\phi_{UC}^{(a)}$ can be reliably measured with the absolute method for a wide range of UC materials, ranging from nanocrystals (NCs) to single crystals, and in different laboratories with slightly differing setups.^[20–22]

In contrast to the absolute method, the relative method does not require an integrating sphere and can be performed using only laser, power meter, spot-size measurement, and a spectrometer. Previously, near-infrared (NIR) absorbing dyes have been used as quantum yield reference in the relative method. For instance, Chen et al. measured the relative UCQY, defined as $\phi_{UC}^{(r)}$, of α -NaYbF₄:Tm³⁺/CaF₂ core/shell NCs using an IR-26 reference dye, which absorbs radiation at $\approx 980\ nm$ and emits at $1130\ nm$ with ϕ of 0.6%.^[23] Two solutions (NCs and dye) with similar optical density of 0.09 at $975\ nm$ are characterized using customized setup consisting of excitation laser, monochromator, and InGaAs photodiodes. The main limitation of the relative method in this case is different emission wavelengths of NCs and the reference dye, which emit at 800 and $1130\ nm$, respectively. Thus, the detector requires accurate calibration as sensitivity of InGaAs photodiodes at $800\ nm$ (Tm³⁺ emission) is much lower than at $1130\ nm$ (IR-26 emission). In addition, the proposed optical setup cannot be used to study Er³⁺ and Ho³⁺ UC emission (observed in the visible range) because InGaAs photodiodes are not designed to detect visible photons. Thus, the relative method is not yet the best choice due to the lack of robust and reliable UC reference materials that emit visible light.

As an alternative to the absolute and relative methods, May et al. present a method that uses the ${}^2F_{5/2} \rightarrow {}^2F_{7/2}$ emission line of Yb³⁺ as an internal standard for determination of ϕ_{UC} .^[24] As the majority of NIR-to-visible UC materials are sensitized with Yb³⁺, this method can be very helpful for a comparison of UC phosphors, although the method requires additional equipment to measure μs – ms time-scale PL decay times.

In this work, the use of nonhygroscopic SrF₂:Yb³⁺,Er³⁺ single crystals as a reference material for determining the UCQY by the relative method is investigated. A single crystal of SrF₂ codoped with Yb³⁺ and Er³⁺ is characterized in an integrating sphere under $976\ nm$ excitation, providing an intensity dependency of $\phi_{UC}^{(a)}$. Then, the SrF₂:Yb³⁺,Er³⁺ single crystal is employed as

a UCQY reference to measure the relative $\phi_{UC}^{(r)}$ of α -NaYF₄:2% Er³⁺;18%Yb³⁺@CaF₂ NCs to address a common question that arises in any laboratory investigating new UC materials: what is quantum yield of newly synthesized UC NCs. As a last step in determining the quantum yield, the $\phi_{UC}^{(a)}$ of α -NaYF₄:2% Er³⁺;18%Yb³⁺@CaF₂ is measured using an integrating sphere and compared the obtained result with the result of the relative method.

2. Experimental Section

2.1. Synthesis of Single Crystal

The single-crystal SrF₂ codoped with 1 mol% of Er³⁺ and 1 mol% of Yb³⁺ (SrF₂:1%Yb³⁺,1%Er³⁺) is synthesized by a methodology reported elsewhere.^[25] Briefly, the fluoride single crystals are grown by Bridgman technique in a vacuum furnace containing CF₄ fluorinating atmosphere. Highly pure fluoride powder precursors, namely, strontium fluoride, ytterbium fluoride, and erbium fluoride (99.99% LANHIT, Russia), are used. The powders are melted in CF₄ atmosphere in advance. Both the heater—with temperature gradient of 60 – $80\ K\ cm^{-1}$ —and crucible are made out of graphite. The grown crystals are $3.5\ cm$ long rods with $0.9\ cm$ diameter. It should be noted that the growth of single crystals based on alkaline earth fluorides doped with rare-earth elements is a well-developed technology, albeit on the laboratory scale.^[26] A typical growth process produces six-single crystals in 8 days, including 1) 1 day for crystal growing and 2) the prefluorination step (melting in CF₄ atmosphere) that takes 1 week. Moreover, Yb³⁺/Tm³⁺ and Yb³⁺/Ho³⁺ codoped single crystals can be obtained after changing the temperature regime according to the corresponding phase diagrams.^[26]

2.2. Synthesis of α -NaYF₄:18%Yb³⁺,2%Er³⁺@CaF₂ NCs

Oleic acid (OA, technical grade, 90%), oleylamine (OAm, technical grade, 70%), 1-octadecene (ODE, technical 90%), trifluoroacetic acid (TFA 99%), and toluene (C₆H₅CH₃) are purchased from Sigma-Aldrich and are used without further purification. Rare-earth trifluoroacetates are synthesized by a methodology reported elsewhere.^[27] All reagents used for the synthesis of the nanoparticles are kept inside a glove box with a N₂ atmosphere.

α -NaYF₄:18%Yb³⁺,2%Er³⁺ NCs are synthesized by a heating-up procedure.^[28] First, NaTFA (1 mmol), Y(TFA)₃ (0.8 mmol), Yb(TFA)₃ (0.18 mmol), and Er(TFA)₃ (0.02 mmol) are added to a mixture of oleic acid, oleylamine, and 1-octadecene (7.4 mL/3.3 mL/3.2 mL) in a round bottom Schleck flask. The solution is purged from oxygen by performing 5 vacuum/Ar cycles at room temperature. Afterward, the mixture is heated up under Ar flow to $110\ ^\circ C$ for 30 min to solubilize the powder, followed by five more vacuum/Ar cycles, and 10 min of dynamic vacuum. The solution is then heated up to $300\ ^\circ C$ for 30 min. After the aging time, the solution is removed from the heating mantle to be cooled down to room temperature. The NCs are extracted by centrifugation ($6796\ \times g$ in Sigma 2-16P centrifuge) with ethanol and acetone several times. Finally, the NCs are dispersed in 1 mL of toluene for storage.

Subsequently, 0.500 μL of $\alpha\text{-NaYF}_4\text{:18\%Yb}^{3+}, 2\%\text{Er}^{3+}$ seeds was mixed with 2 mmol $\text{Ca}(\text{TFA})_2$, in a 1-octadecene/oleic acid solution (7 mL/7 mL). The new mixture was purged also from air by performing 5 vacuum/Ar cycles at room temperature. Then, the mixture was heated under Ar flow to 120 $^\circ\text{C}$ for 30 min to solubilize the $\text{Ca}(\text{TFA})_2$, followed by five more vacuum/Ar cycles, and 10 min of dynamic vacuum. The solution was heated to 300 $^\circ\text{C}$ for 45 min. After aging, the solution was cooled down to room temperature. The core/shell NCs were extracted by the same procedure described above for the core NCs, and dispersed in 1 mL of toluene for storage.

2.3. Characterization of NCs

The size distribution and morphology of the NCs is studied by a high-angle annular dark field (HAADF) scanning transmission electron microscopy (STEM) conducted with FEI Osiris Chemi STEM microscope at 200 keV (see Figure S1, Supporting Information). In addition, phase identification of synthesized NCs (Figure S2, Supporting Information) is performed with X-ray diffractometer (XRD, Bruker D2 Phaser) using Cu $K\alpha$ radiation ($\lambda = 1.5405 \text{ \AA}$).

2.4. Preparation of Reference UC Sample

Figure S3, Supporting Information, illustrates the cylindrical $\text{SrF}_2\text{:1\%Yb}^{3+}, 1\%\text{Er}^{3+}$ ingot which is cut along the long axis into a parallelepiped with dimensions ($3 \times 3 \times 20 \text{ mm}$). The parallelepiped is polished to reduce scattering in three steps. Each side is first treated with a polishing paper with grit number P1200 ($15.3 \mu\text{m}$) and then with P4000 polishing paper ($5.0 \mu\text{m}$) and finally finished with a grit 14 000 ($1 \mu\text{m}$) polishing disc. A crystal width of $d = 3 \text{ mm}$ was considered to be close to the optimum width of the reference crystal because: 1) the crystal must be compatible with commercially available cuvettes such as type 22.3/Q (Starna) that fit into a standard spectrometer cuvette holder; and 2) the width of the crystal must be greater than the diameter of the light beam in the spectrophotometer when measuring absorption spectra and the laser beam when measuring UC spectra. For these reasons, a crystal with $d = 3 \text{ mm}$ was preferred over crystals with $d = 1 \text{ mm}$ or $d = 2 \text{ mm}$. If required in the future, a wider ($d = 5 \text{ mm}$) crystal can also be provided as a reference crystal, in combination with cuvette type 3–5.45 (Starna) and adapter FCA5 (Starna).

2.5. Optical Characterization

Absorption spectra are recorded using an ultraviolet/visible/near-infrared (UV/vis/NIR) spectrophotometer (Perkin Elmer Lambda 950). The absorption coefficient is calculated using Equation (1)

$$\alpha = -\frac{1}{d} \times \ln(10^A) \quad (1)$$

where α is the absorption coefficient in cm^{-1} , A is the absorbance data obtained from the instrument, and d is the sample thickness in centimeters.

A tunable continuous-wave (CW) Ti-sapphire laser (Solstis, M-Squared Lasers Ltd.) pumped by 532 nm laser (Verdi-V18,

Coherent) is used in absolute and relative methods for measurements of UCQY. The maximum output power of the Ti-sapphire laser is tuned to 200 mW at 976 nm. The laser has $<64 \text{ pm}$ bandwidth as well as Gaussian beam profile with beam size $2.38 \times 3.30 \text{ mm}$ (Figure S4a, Supporting Information). To achieve higher intensity of excitation beam, the laser is focused using a lens with 40 cm focal length into spot with size of $0.73 \times 1.12 \text{ mm}$ (Figure S4b, Supporting Information). The size of the laser beam is measured with a beam profiler (Thorlabs, BP209-IR/M) as the distance between two points of intensity distribution, which is $1/e^2 = 0.135$ of the maximum value. The excitation intensity is defined as the ratio of the laser power to the beam area. The uncertainty in determining the laser power is estimated from 10 repeated measurements. The results show that the relative error of the measurement is 1%. This is in agreement with the technical description of the Si-power detector used (S121C, Thorlabs), which states that the uncertainty should not exceed 3%. The same approach is used to estimate the uncertainty of the beam area determination. The beam profile is determined 10 times and the results show that the uncertainty is also 1%. Thus, according to the error propagation method, the relative error of the laser intensity is 1.4%.

2.5.1. Absolute Quantum Yield

The absolute method for the quantum yield characterization is based on the measurement of the number of absorbed and emitted photons, N_a and N_e , respectively (Equation (2))

$$\phi_{\text{UC}}^{(a)} = \frac{N_e}{N_a} \quad (2)$$

When estimating the number of emitted and absorbed photons in the integrating sphere, there are several details to consider. After passing through the sample, the remaining excitation light gets reflected multiple times inside the integrating sphere. For Stokes PL, this can lead to two effects: it 1) increases number of the absorbed photons; and 2) based on this increased absorption also provides an additional number of emitted photons. For UC PL, only the first effect should be considered, as due to the nonlinear intensity dependence of the UCQY the scattered light with a weak intensity does not generate UC PL. To mitigate the first effect, a method based on three measurements (known as 3M), as detailed in Equation (3),^[29] is utilized and instead of Equation (2)

$$\phi_{\text{UC}}^{(a,\text{exp})} = \frac{\text{PD} - \frac{\text{LD}}{\text{LI}} \times \text{PI}}{\left(1 - \frac{\text{LD}}{\text{LI}}\right) \times \text{ES}} \quad (3)$$

where PD is an acronym for PL direct and is attributed to the number of PL photons emitted under direct excitation of the sample, PI stands for PL indirect and is the number of PL photons emitted under indirect excitation, ES is an acronym for empty sphere and is the number of excitation photons measured in empty sphere (without a sample), LD (laser direct) is the number of excitation photons measured at direct excitation of the sample, and LI (laser indirect) is the number of excitation

photons measured at indirect excitation of the sample. Note that to obtain the internal quantum yield $\phi_{UC}^{(a)}$ independent from the sample geometry, the value $\phi_{UC}^{(a,exp)}$ requires an additional correction, which will be described in detail later in the Section 3.

The setup and the methodology for estimation of $\phi_{UC}^{(a,exp)}$ under 976 nm excitation is displayed in Figure S5, Supporting Information. Briefly, the sample is placed inside of an integrating sphere (Labsphere, 6" Ø, 3P-LPM-060-SL) and excited with a laser. A continuously variable neutral density filter wheel (Thorlabs, NDC-100C-2) is used to change excitation intensity. For the measurement of the laser beam size, the beam profiler (Thorlabs, BP209-IR/M) is placed in the same location as the sample. The PL from inside the integrating sphere (PD and PI) is directed to a CCD spectrometer (Thorlabs, CCS200/M) using an optical fiber (BYF105HS02, Thorlabs with diameter 105 µm) in combination with a 950 nm short-pass filter (Semrock, FF01-950/SP-25). The 950 nm short-pass filter is removed for measurements of ES, LD, and LI.

2.5.2. Relative Quantum Yield

The relative method of quantum yield determination is based on a comparison of the emission intensities measured at exactly same excitation and collection conditions for a sample under investigation and a sample with earlier reported ϕ_{ref} (reference sample) using Equation (4)

$$\phi_{UC}^{(r)} = \phi_{ref} \left(\frac{A_{ref}}{A_{UC}} \right) \left(\frac{E_{UC}}{E_{ref}} \right) \left(\frac{n_{UC}}{n_{ref}} \right)^2 \quad (4)$$

where ϕ_{ref} is UCQY of the UC reference, A_{UC} and A_{ref} are the absorbance of UC sample and the UC reference at excitation wavelength, respectively, E_{UC} and E_{ref} represent the integrated PL intensity of the UC sample and the UC reference, respectively, while n_{UC} and n_{ref} are the refractive indexes of the UC sample and the reference sample at the emission wavelength.

For the application of the relative method, the single crystal (having a parallelepiped shape) is placed into a square quartz cuvette (Starna, type 22.3/Q)—with external dimensions of 12.5 × 12.5 mm and a height of 45 mm and an internal size of 3 × 3 mm—and then filled with toluene. This procedure helps to match the refractive indexes and to keep the same size of

the excitation spot and the same PL escape cone for the reference material and a liquid dispersion of UC NCs with unknown quantum yield. The NC sample is also placed into the same cuvette. In both cases, the cuvettes are then placed into a cuvette holder (taken from Agilent Cary Eclipse Fluorescence Spectrometer) mounted onto an optical table. The UC PL is collected using an optical fiber (BYF105HS02, Thorlabs with diameter 105 µm) at the distance of 10 cm from the cuvette and at an angle of 90° relative to the propagation of the excitation laser beam. The optical fiber is connected to a CCD spectrometer (Thorlabs, CCS200/M) for measurements of PL spectra. The schematic of the setup for estimation of $\phi_{UC}^{(r)}$ is presented in Figure S6, Supporting Information.

3. Results and Discussion

The absorption spectrum of the SrF₂:1%Yb³⁺, 1%Er³⁺ single crystal is plotted in Figure 1a, which consists of the prominent peaks of Yb³⁺ and Er³⁺ ions. The most intense absorption band is observed between 900 and 1000 nm, which corresponds to a superposition of the Yb³⁺:²F_{7/2} → ²F_{7/2} and Er³⁺:⁴I_{15/2} → ⁴I_{11/2} transitions. The absorption coefficient at λ_{max} = 976 nm reaches 1.74 cm⁻¹, which means that the studied sample with 3 mm thickness can absorb 39% of incident photons. The excitation of the crystal with 976 nm laser results in strong UC emission detected in the visible spectral range. Figure 1b displays UC PL spectra with three major peaks corresponding to Er³⁺:²H_{11/2} & ⁴S_{3/2} → ⁴I_{15/2} (green), Er³⁺:⁴F_{9/2} → ⁴I_{15/2} (red), and Er³⁺:⁴S_{3/2} → ⁴I_{13/2} (NIR) transitions.

The UC PL of the crystal is characterized via quantification of $\phi_{UC}^{(a,exp)}$ using the absolute method. The crystal in the quartz cuvette is placed inside an integrating sphere and $\phi_{UC}^{(a,exp)}$ is measured over the spectral range 500–875 nm for different excitation intensities (as depicted in Figure 2). Even at relatively low excitation intensity of 1 W cm⁻², the UC demonstrates reasonably high efficiency with $\phi_{UC}^{(a,exp)}$ of 0.08%. The $\phi_{UC}^{(a,exp)}$ value increases gradually with the rise of intensity and saturates at excitation intensity of 200 W cm⁻². At this intensity a value of $\phi_{UC}^{(a,exp)} = 7.6\%$ is achieved. Note that the absolute errors for $\phi_{UC}^{(a,exp)}$ in Figure 2 are obtained as a standard deviation of five measurements (for each measurement, the crystal is removed from the integrating sphere and then placed back inside).

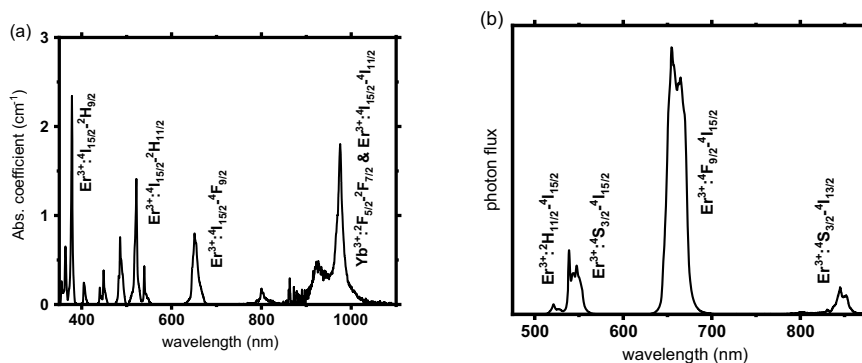


Figure 1. a) Absorption coefficient of the SrF₂:1%Yb³⁺, 1%Er³⁺ sample; b) UC emission spectrum of the SrF₂:1%Yb³⁺, 1%Er³⁺ crystal under 976 nm excitation (10 W cm⁻²).

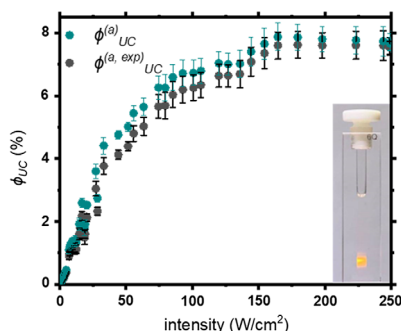


Figure 2. Intensity dependence of the absolute UCQY in the 400–900 nm range of the SrF₂:1%Yb³⁺,1%Er³⁺ single crystal under 976 nm excitation. Black circles show $\phi_{UC}^{(a,exp)}$ values as measured in the integrating sphere using the 3M method and turquoise circles represent $\phi_{UC}^{(a)}$ values after the correction using Equation (5). The photograph (inset) shows the reference crystal in a 12.5 × 12.5 mm quartz cuvette (with 3 × 3 mm inner space) under 976 nm excitation taken in daylight using a smartphone camera (Apple iPhone 10).

The following analysis demonstrates that measurements using an integrating sphere can slightly underestimate the UCQY and four possible sources for this deviation are identified:

First, the photons which are not absorbed by the crystal after direct excitation can be many times reflected by the integration sphere and absorbed by the crystal inducing secondary (indirect) absorption. As previously mentioned, this indirect absorption does not result in any significant UC PL due to the much lower intensity of the now-scattered beam. However, this phenomenon does lead to an apparent increase of absorption and, thus, reduces $\phi_{UC}^{(a,exp)}$ as compared to quantum yield $\phi_{UC}^{(a)}$, which can be expected outside an integrating sphere. In this case, a measurement correction can be performed using the so-called 3M method^[29,30] (Equation (3)), which includes effects of indirect absorption as described earlier in Section 2.

Second, similar to excitation photons, the emitted photons can also be reflected inside the integrating sphere, which causes them to repeatedly pass through the crystal and undergo reabsorption. Critically, the transition Er³⁺:⁴S_{3/2} → ⁴I_{13/2} (at 845 nm) is not subject to reabsorption because it is a transition between two excited states (and the population density of the low-lying excited state is always negligible compared to the ground state density). Taking advantage of this, two measurements can be performed—namely, with and without the integrating sphere (with a fixed excitation and detection scheme)—that then allow for the percentage of reabsorbed light inside the integrating sphere to be estimated, assuming that the intensity of the luminescent peak corresponding to the ⁴S_{3/2} → ⁴I_{13/2} transition is unchanged. Figure S7, Supporting Information, indicates that at the chosen Er³⁺ concentration (1 mol%), the reabsorption for the ⁴F_{9/2} → ⁴I_{15/2} transition is only 0.5% (the relative change in intensity of peak measured inside and outside the integrating sphere), whereas about 1.7% (relative change) is observed for the ²H_{11/2} & ⁴S_{3/2} → ⁴I_{15/2} transition. Thus, the correction coefficients ($a = 0.995$ (²H_{11/2} & ⁴S_{3/2} → ⁴I_{15/2}), $a = 0.983$ (⁴F_{9/2} → ⁴I_{15/2}), and $a = 1.000$ (²H_{11/2} & ⁴S_{3/2} → ⁴I_{13/2})) should be introduced to

approach quantum yield $\phi_{UC}^{(a)}$ corrected for reabsorption (see Equation (5)). Furthermore, PL can also be reabsorbed in the experiment performed without the integrating sphere. However, for this case (without multiple passes of emitted photons through the crystal) the level of reabsorption is $\ll 0.1\%$ (relative change) and hence did not require an additional correction.

Third, reason for underestimating of $\phi_{UC}^{(a)}$ is derived from nonlinear origin of the UC process—dependency of UC yield on the excitation intensity ($\phi_{UC} = I^{n-1}$). For a crystal with a finite thickness, the excitation intensity decreases as light propagates through the crystal. Therefore, the thinner crystal should exhibit higher $\phi_{UC}^{(a,exp)}$. A result of numerical simulation presented in Figure S8b,c, Supporting Information, indicates that for the reference 3 mm crystal with absorptance of 39%, the measured value of $\phi_{UC}^{(a,exp)}$ is smaller than internal UC quantum yield (ϕ_{UC}^a) and difference between $\phi_{UC}^{(a,exp)}$ and ϕ_{UC}^a depends on excitation intensity. For instance, for the ⁴F_{9/2} → ⁴I_{15/2} transition, the $\phi_{UC}^{(a,exp)}$ value can be underestimated by a factor of 0.83 at low intensity (1 W cm⁻²), when $\phi_{UC} = I^{1.0}$ and by a factor of 0.97 at high intensities (250 W cm⁻²) when $\phi_{UC} = I^{0.1}$. The slightly smaller factor of 0.95 is obtained for the ²H_{11/2} & ⁴S_{3/2} → ⁴I_{15/2} transition at 250 W cm⁻² because $\phi_{UC} = I^{0.2}$. Thus, in order obtain $\phi_{UC}^{(a)}$ corrected for reduction in excitation intensity as light propagates through the crystal, an additional correction—realized via a correction coefficient b —is required and is implemented in Equation (5).

Fourth, possible reason leading to underestimation of $\phi_{UC}^{(a)}$ is local heating within the excitation spot, as reported by Joseph et al. for micropowder samples.^[31] The heating effect may require additional correction for temperature realized by using a correction coefficient c in Equation (5). The local temperature can be conveniently probed using the ratio of PL for two thermally coupled Er³⁺ levels, namely, ²H_{11/2} and ⁴S_{3/2}. An increase of local temperature leads to increase of the intensity ratio of the ²H_{11/2} → ⁴I_{15/2} and ²S_{3/2} → ⁴I_{15/2} transitions. However, Figure S9a, Supporting Information, indicates that this ratio stays almost unchanged over the entire range 0.1–250 W cm⁻², revealing very good thermal conductivity of the used crystals compared to micropowders where heating is more likely to be a problem.^[32] Thus, the increase in the temperature of the single-crystal sample is not detected (Figure S9b, Supporting Information) and the data do not require temperature correction ($c = 1$).

In general, the use of the 3M experimental method and the three correction factors a , b , and c in Equation (5) are applied to obtain values of $\phi_{UC}^{(a)}$ for the reference crystal

$$\phi_{UC}^{(a)} = \frac{\phi_{UC}^{(a,exp)}}{a \cdot b \cdot c} \quad (5)$$

where $\phi_{UC}^{(a,exp)}$ is the experimental value of UCQY, a is a correction factor due to reabsorption of UC emission in the integrating sphere (Figure S7, Supporting Information), while b is a correction factor due to the finite thickness of the sample changing the excitation power with depth into the sample and the nonlinear origin of UC (Figure S8, Supporting Information) and c is

correction factor due to temperature change (Figure S9, Supporting Information).

Figure 2 displays the intensity dependence of the quantum yield $\phi_{UC}^{(a)}$ obtained via correction of experimental values of quantum yield $\phi_{UC}^{(a,exp)}$ using Equation (5). Note that the quantum yield correction is performed for the green (${}^2H_{11/2}&{}^4S_{3/2}\rightarrow{}^4I_{15/2}$), red ($Er^{3+}:{}^4F_{9/2}\rightarrow{}^4I_{15/2}$), and NIR (${}^2H_{11/2}&{}^4S_{3/2}\rightarrow{}^4I_{13/2}$) UC emission peaks separately (Figure S10, Supporting Information), whereas Figure 2 displays total UCQY after summing up quantum yields of the individual transitions. For instance, the intensity dependency of $\phi_{UC}^{(a)}$ demonstrates its rise from 0.1% at 1 W cm^{-2} to 1.4% at 10 W cm^{-2} and further to 7.6% at 250 W cm^{-2} . The absolute error of $\phi_{UC}^{(a)}$ in Figure 2 is calculated using the assumption that both parameter $\phi_{UC}^{(a)}$ and $\phi_{UC}^{(a,exp)}$ have the same relative error.

As NCs are the most intensively investigated class of UC materials,^[33,34] a NC-based UC system is chosen for a comparison of the absolute method and the relative method; the latter using the reference $SrF_2:1\%Yb^{3+},1\%Er^{3+}$ single crystal. The NC sample, with a $\alpha\text{-NaYF}_4:18\%Yb^{3+},2\%Er^{3+}@CaF_2$ core@shell structure, is chosen for a number of reasons. On the one hand, $\alpha\text{-NaYF}_4$ NCs codoped with different lanthanide ions demonstrate great potential in synthesis of new bright UC core/shell NCs, especially when the surface is passivated by an optically inert shell, like CaF_2 .^[35–37] On the other hand, the UC emission in $\alpha\text{-NaYF}_4:18\%Yb^{3+},2\%Er^{3+}@CaF_2$ NCs is defined by Er^{3+} ions which makes it easy to compare it to the reference material (Figure 3a).

In order to use the relative method to measure the UC quantum yield, both the reference and the sample must be characterized outside the integrating sphere. Thus, the question arises whether it is correct to take the UCQY values obtained for the $SrF_2:1\%Yb^{3+},1\%Er^{3+}$ reference crystal inside the integrating sphere and apply them in Equation (4)? To answer this, one needs to consider the one main difference between measurements inside and outside the integrating sphere—stronger reabsorption of emitted photons inside the integrating sphere due to multiple pass through the $SrF_2:1\%Yb^{3+},1\%Er^{3+}$ crystal. Therefore, the correction must be applied: $\phi_{ref} = \phi_{UC}^{(a,exp)}/a$. However, it has previously been shown that the correction

parameter a for the $SrF_2:1\%Yb^{3+},1\%Er^{3+}$ crystal is very close to unity ($a = 0.995$ for the $Er^{3+}:{}^2H_{11/2}&{}^4S_{3/2}\rightarrow{}^4I_{15/2}$ transition, $a = 0.983$ for the $Er^{3+}:{}^4F_{9/2}\rightarrow{}^4I_{15/2}$ transition, and $a = 1$ for the $Er^{3+}:{}^2H_{11/2}&{}^4S_{3/2}\rightarrow{}^4I_{13/2}$ transition), which leads to $\phi_{ref} = \phi_{UC}^{(a,exp)}$ in good approximation for all excitation intensities.

Four additional parameters need to be known to apply Equation (4), namely, absorbance of the reference (A_{ref}) and the studied material (A_{UC}) at 976 nm, as well as integral PL intensity as function of excitation intensity of the reference (E_{ref}) and the studied material (E_{UC}). The refractive indexes of toluene and SrF_2 in the range 520–650 nm are 1.503–1.492^[38] and 1.439–1.437,^[39] respectively. The ratio of $\left(\frac{n_{UC}}{n_{ref}}\right)^2$ is therefore 1.04 and Equation (4) can be simplified as

$$\phi_{UC}^{(r,exp)} = 1.04\phi_{UC}^{(a,exp)}\left(\frac{A_{ref}}{A_{UC}}\right)\left(\frac{E_{UC}}{E_{ref}}\right) \quad (6)$$

The A_{ref} for the $SrF_2:1\%Yb^{3+},1\%Er^{3+}$ crystal and A_{UC} for $\alpha\text{-NaYF}_4:18\%Yb^{3+},2\%Er^{3+}@CaF_2$ NCs are measured using two methods: 1) UV/vis/NIR spectrometer (Figure S11, Supporting Information) and 2) integrating sphere, where the absorbance is calculated as ratio between laser intensity $(1 - \frac{I}{I_0})$ in Equation (3). Both methods provide similar results, with absorbance of the reference being $A_{ref} = 39\%$ and the NC sample being $A_{UC} = 7\%$. The coincidence of the results of two methods confirms that absorbance of reference crystals and UC NCs can be reliably measured in a cuvette with the 3 mm beam path using standard UV/vis/NIR spectrometer. As a word of caution to the interested reader, due to a small inner size of the cuvette (3 mm), method (1) might underestimate the absorbance. This will occur if the light beam in the spectrometer is larger than the inner size of the cuvette (in the present case > 3 mm). The beam size can be checked in a simple way by setting the spectrometer to light at about 550 nm (i.e., where the eye is very sensitive) and observing with the naked eye. Further, the beam size should be controlled using either settings of a UV/vis/NIR spectrometer or by placing an adjustable diaphragm at the monochromator exit.

Knowing all these values now allows the intensity dependence $\phi_{UC}^{(r,exp)}$ to be calculated (Figure 3b). At a relatively low excitation intensity of 1 W cm^{-2} , the UC demonstrates reasonably high

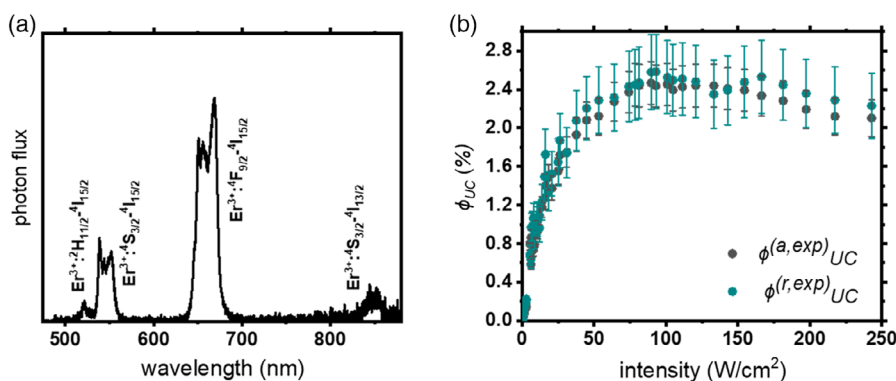


Figure 3. a) UC emission spectrum of $\alpha\text{-NaYF}_4:18\%Yb^{3+},2\%Er^{3+}@CaF_2$ NCs under 976 nm excitation (289 W cm^{-2}); b) intensity dependence of $\phi_{UC}^{(a,exp)}$ and $\phi_{UC}^{(r,exp)}$ of $\alpha\text{-NaYF}_4:18\%Yb^{3+},2\%Er^{3+}@CaF_2$ NCs under 976 nm excitation in the $0.1\text{--}250\text{ W cm}^{-2}$ intensity range.

efficiency with $\phi_{UC}^{(r,exp)}$ of 0.09%. The $\phi_{UC}^{(r,exp)}$ value increases gradually with the rise of intensity to 1.1% (at 10 W cm^{-2}) and reaches 2.5% at 100 W cm^{-2} . Comparing the relative UC quantum yield results to those obtained via the absolute method (Figure 3b and S10a,b, Supporting Information), at an excitation intensity of 1 W cm^{-2} , the UC demonstrates $\phi_{UC}^{(a,exp)}$ of 0.06%. At 10 W cm^{-2} , the $\phi_{UC}^{(r,exp)}$ value increases gradually to 0.9% and reaches 2.4% at 100 W cm^{-2} . Overall, a very good overlap exists between the results of the relative and absolute methods. Note that the absolute errors for $\phi_{UC}^{(a,exp)}$ in Figure 3b are obtained as a standard deviation of five measurements (for each measurement, the cuvette is removed from the integrating sphere and then placed back inside). As $\phi_{UC}^{(r,exp)}$ is estimated using four independent measurements (two different materials—reference crystal and sample, and two different devices—UV/vis/NIR spectrometer and fluorescence spectrometer), the error in the estimate of $\phi_{UC}^{(r,exp)}$ (Figure 3b) is calculated using error propagation analysis, with a description of the method is detailed in the Section S14, Supporting Information.

As UC is nonlinear process, the accuracy ϕ_{UC} for both the absolute and relative methods depends on the excitation intensity and the sample absorbance. For instance, Figure 4a demonstrates the experimental relative difference between $\phi_{UC}^{(r,exp)}$ and $\phi_{UC}^{(a,exp)}$ calculated for various excitation intensities. Very good agreement is observed between the UCQYs (with a relative difference of $\approx 5\%$) for high excitation intensity ($>10 \text{ W cm}^{-2}$). In contrast, the quantum yield values exhibit a larger difference of $\approx 24\%$ for low excitation intensity, when $\phi_{UC}^{(a,exp)}$ and $\phi_{UC}^{(r,exp)}$ are less than 0.7%. It can be assumed that there may be additional systematic error when measuring inside an integrating sphere with an unfocused beam ($<10 \text{ W cm}^{-2}$), so that a small deviation in the position of the sample inside the integrating sphere can slightly alter the excitation intensity (Figure S4, Supporting Information).

In general, the observed differences are surprisingly good considering the accuracy of the measurements presented as error bars in Figure 3b. It is therefore expected that, given the very good overlap between the methods used, the proposed relative method for estimating the quantum yield of UC NCs can find widespread application in the research labs worldwide.

Furthermore, a theoretical analysis of uncertainty in absolute and relative methods can be also performed via error propagation analysis. As has been discussed in work by Leyre et al.,^[40] the absorbance measurement usually introduces the biggest error into quantum yield measurements. Figure 4b compares relative error $\delta(\phi_{UC})$ in the UCQY measured by the absolute and relative methods as the function of the absorbance (see Section S14, Supporting Information, for details). The results of the calculation indicate that for samples with weak absorption (absorbance $<7\%$) the relative method provides slightly smaller uncertainty in UC quantum yield. In contrast, for a more strongly absorbing sample (absorbance $>7\%$), the absolute method can provide more precise measurement of UCQY. For the values of absorbance of 39% for the $\text{SrF}_2:1\% \text{Yb}^{3+}, 1\% \text{Er}^{3+}$ crystal and 7% for $\alpha\text{-NaYF}_4:18\% \text{Yb}^{3+}, 2\% \text{Er}^{3+} @ \text{CaF}_2$ NCs, the values of the relative error are calculated equal to $\delta(\phi_{UC}^{(a,exp)}) = 3\%$ (for the crystal), $\delta(\phi_{UC}^{(a,exp)}) = 18\%$, and $\delta(\phi_{UC}^{(r,exp)}) = 18\%$ (for the NCs). Therefore, again a very good overlap between uncertainties obtained via theoretical analysis and repeated measurements is observed. Figure 4b indicates that there is a certain limit in sample absorbance required for estimation of UC QY. For a sample with an absorbance below 3%, the uncertainty increases to 50% or more, regardless of the method. Although the uncertainty decreases with increasing absorbance, for strongly absorbing samples (with absorbance $>50\%$), the measured UC quantum yield becomes sample dependent and severe correction (Equation (5)) is required to obtain $\phi_{UC}^{(a)}$. The detailed discussion of such a correction was presented earlier for $\text{SrF}_2:1\% \text{Yb}^{3+}, 1\% \text{Er}^{3+}$ crystal with absorbance of 39% (Figure 2). In turn, the experimental values from Figure 3b should be also corrected using Equation (5) to obtain the UCQY of the NCs. As the NC dispersion exhibits a low absorbance (7%), the correction leads to very little change in quantum yields, as shown in Figure S12, Supporting Information, for the QY estimated with the both methods and $\phi_{UC}^{(a,exp)} = \phi_{UC}^{(a)}$.

It should be noted that the NIR laser excitation for UC measurements is not always performed at 976 nm. The lasing wavelength can range from 970 to 980 nm. Obviously, the dependence of the UCQY on the intensity changes with the excitation wavelength because the internal UCQY is proportional to the number of absorbed photons. In turn, the number of absorbed photons

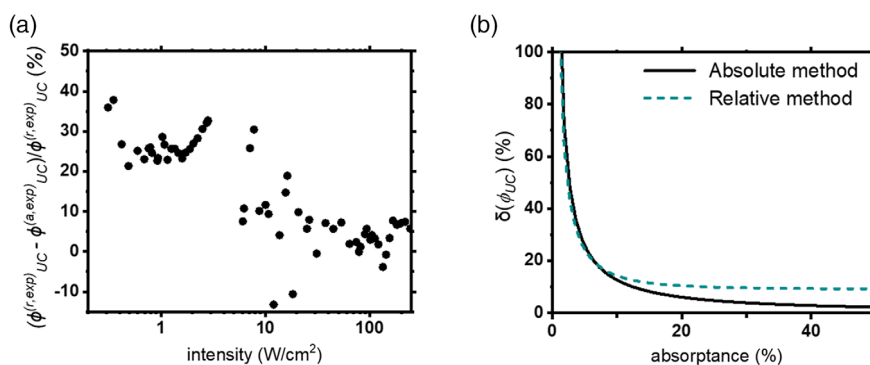


Figure 4. a) Discrepancy between $\phi_{UC}^{(a,exp)}$ and $\phi_{UC}^{(r,exp)}$ as a function of excitation intensity; b) relative error of the determination of ϕ_{UC} in the absolute and relative methods as a function of sample absorbance.

varies with wavelength at the same excitation intensity. Accounting for the difference in the number of absorbed photons, the intensity dependence $\phi_{UC}^{(a,exp)}$ is measured for the SrF₂:1%Yb³⁺,1%Er³⁺ crystal for several typical excitation wavelengths (Figure S13, Supporting Information). The $\phi_{UC}^{(a,exp)}$ dependency on the excitation wavelength demonstrates the highest values of UCQY at 976 nm excitation (that corresponds to the position of absorption peak), whereas the slightly lower $\phi_{UC}^{(a,exp)}$ values are found for 974, 978, and 980 nm excitation wavelengths. The lowest values of $\phi_{UC}^{(a,exp)}$ are observed for 979 and 972 nm excitation wavelengths. Thus, these reference curves can be also used in the relative method if an excitation wavelength other than 976 nm is used for the optical characterization of UC NCs.

4. Conclusions

Dependence of UCQY on excitation intensity for SrF₂:1%Yb³⁺, 1%Er³⁺ crystal with absorptance of 39% at 976 nm is measured in an integrating sphere. It is found that measurements of the crystal with high absorptance in the integrating sphere underestimate values of UCQY due to several factors. A simple equation is proposed for the UCQY correction, including correction for reabsorption, correction for reduction in excitation intensity as light propagates through the crystal, and correction for temperature change. The application of the SrF₂:1%Yb³⁺,1%Er³⁺ crystal as an UCQY reference material is investigated. The UCQY of α -NaYF₄:18%Yb³⁺, 2%Er³⁺@CaF₂ NCs dispersed in toluene is performed with the relative method using the SrF₂:1%Yb³⁺, 1%Er³⁺ crystal and with the absolute method in an integrating sphere. These two measurements exhibit an excellent level of conformity, resulting in quantum yield values of $\phi_{UC}^{(r)} = 2.5\%$ and $\phi_{UC}^{(a)} = 2.4\%$ at 976 nm excitation with intensity of 100 W cm⁻², respectively. Furthermore, intensity dependencies of UCQY for α -NaYF₄:18%Yb³⁺, 2%Er³⁺@CaF₂ NCs were investigated in the range 0.1–250 W cm⁻² using absolute and relative methods, and a very good match is found for both methods.

Overall, it is anticipated that it will be very convenient to have the reference SrF₂:1%Yb³⁺, 1%Er³⁺ crystal in a laboratory if either absolute or relative methods are used to measure UC quantum yield. In case of the absolute method, the accuracy of the measurement depends on many factors: 1) correct measurements of parameters described in Equation (3); 2) proper calibration of the optical system, due to replacing or changing the position of each individual part, such as fibers, beam splitters, and spectrometer slits, along with changes to the calibration of the optical system used; and 3) correct estimation of excitation intensity on the sample inside the integrating sphere. Thus, even if the absolute method is used, the reference UC crystal can ensure that there are no systematic errors and to prove the validity of quantum yield measurements in daily routine measurements.

In the context of relative quantum yield measurements, it has been demonstrated that the reference crystal can be placed in a standard 1 cm quartz cuvette, which is often used in characterization of UC NCs. Thus, to measure $\phi_{UC}^{(r)}$ UC NCs using the

reference single crystal, relatively simple optical equipment can be used, including an excitation laser, a standard cuvette holder (in 90° measurement geometry), and a compact CCD spectrometer.

Supporting Information

Supporting Information is available from the Wiley Online Library or from the author.

Acknowledgements

The reported study was funded by RFBR (project no. 21-53-12017 for S.V.K., V.A.K., A.N.N., and A.A.A.) and DFG (project no. TU 487/8-1 for A.T. and B.S.R.). The authors acknowledge Project DEAL for open access funding. The financial support provided by the Helmholtz Association is gratefully acknowledged: 1) a Recruitment Initiative Fellowship for B.S.R.; 2) the funding of chemical synthesis equipment from the Helmholtz Materials Energy Foundry (HEMF); and 3) Research Field Energy—Program Materials and Technologies for the Energy Transition—Topic 1 Photovoltaics. The authors acknowledge R. Popescu (LEM, KIT) for conducting scanning transmission electron microscopy.

Conflict of Interest

The authors declare no conflict of interest.

Data Availability Statement

The data that support the findings of this study are available from the corresponding author upon reasonable request.

Keywords

nanocrystals, photoluminescence quantum yield, rare-earth ions, single crystal, upconversion

Received: June 24, 2022
Revised: November 17, 2022
Published online:

- [1] H. Wu, Z. Hao, L. Zhang, X. Zhang, Y. Xiao, G.-H. Pan, H. Wu, Y. Luo, H. Zhao, J. Zhang, *J. Phys. Chem. C* **2018**, 122, 9611.
- [2] M.-Q. Yang, M. Gao, M. Hong, G. W. Ho, *Adv. Mater.* **2018**, 30, 1802894.
- [3] B. S. Richards, D. Hudry, D. Busko, A. Turshatov, I. A. Howard, *Chem. Rev.* **2021**, 121, 9165.
- [4] M. Runowski, N. Stopikowska, D. Szeremeta, S. Goderski, M. Skwierczyńska, S. Lis, *ACS Appl. Mater. Interfaces* **2019**, 11, 13389.
- [5] X. Liu, Q. Ji, Q. Hu, C. Li, M. Chen, J. Sun, Y. Wang, Q. Sun, B. Geng, *ACS Appl. Mater. Interfaces* **2019**, 11, 30146.
- [6] C. Würth, M. Grabolle, J. Pauli, M. Spieles, U. Resch-Genger, *Nat. Protocols* **2013**, 8, 1535.
- [7] C. Würth, D. Geißler, T. Behnke, M. Kaiser, U. Resch-Genger, *Anal. Bioanal. Chem.* **2015**, 407, 59.
- [8] K. Rurack, in *Standardization And Quality Assurance In Fluorescence Measurements I: Techniques* (Ed: U. Resch-Genger), Springer Berlin

- Heidelberg, Berlin, Heidelberg **2008**, p. 101, https://doi.org/10.1007/4243_2008_019.
- [9] L. Porrès, A. Holland, L.-O. Pålsson, A. P. Monkman, C. Kemp, A. Beeby, *J. Fluoresc.* **2006**, *16*, 267.
- [10] C. Würth, M. G. González, R. Niessner, U. Panne, C. Haisch, U. R. Genger, *Talanta* **2012**, *90*, 30.
- [11] B. Amouroux, C. Roux, J.-C. Micheau, F. Gauffre, C. Coudret, *Beilstein J. Org. Chem.* **2019**, *15*, 2671.
- [12] J. Olmsted, *J. Phys. Chem.* **1979**, *83*, 2581.
- [13] D. O. Faulkner, S. Petrov, D. D. Perovic, N. P. Kherani, G. A. Ozin, *J. Mater. Chem.* **2012**, *22*, 24330.
- [14] S. Fischer, B. Fröhlich, K. W. Krämer, J. C. Goldschmidt, *J. Phys. Chem. C* **2014**, *118*, 30106.
- [15] S. Fischer, N. J. J. Johnson, J. Pichaandi, J. C. Goldschmidt, F. C. J. M. V. Veggel, *J. Appl. Phys.* **2015**, *118*, 193105.
- [16] M. Kaiser, C. Würth, M. Kraft, I. Hyppänen, T. Soukka, U. Resch-Genger, *Nanoscale* **2017**, *9*, 10051.
- [17] I. N. Stanton, J. A. Ayres, J. T. Stecher, M. C. Fischer, D. Scharpf, J. D. Scheuch, M. J. Therien, *J. Phys. Chem. C* **2018**, *122*, 252.
- [18] C. Homann, L. Krukewitt, F. Frenzel, B. Grauel, C. Würth, U. Resch-Genger, M. Haase, *Angew. Chem. Int. Ed.* **2018**, *57*, 8765.
- [19] M. Kaiser, C. Würth, M. Kraft, T. Soukka, U. Resch-Genger, *Nano Res.* **2019**, *12*, 1871.
- [20] M. S. Meijer, P. A. Rojas-Gutierrez, D. Busko, I. A. Howard, F. Frenzel, C. Würth, U. Resch-Genger, B. S. Richards, A. Turshatov, J. A. Capobianco, S. Bonnet, *Phys. Chem. Chem. Phys.* **2018**, *20*, 22556.
- [21] D. Saleta Reig, B. Grauel, V. A. Konyushkin, A. N. Nakladov, P. P. Fedorov, D. Busko, I. A. Howard, B. S. Richards, U. Resch-Genger, S. V. Kuznetsov, A. Turshatov, C. Würth, *J. Mater. Chem. C* **2020**, *8*, 4093.
- [22] C. D. S. Brites, S. V. Kuznetsov, V. A. Konyushkin, A. N. Nakladov, P. P. Fedorov, L. D. Carlos, *Eur. J. Inorg. Chem.* **2020**, *2020*, 1555.
- [23] G. Chen, J. Shen, T. Y. Ohulchanskyy, N. J. Patel, A. Kutikov, Z. Li, J. Song, R. K. Pandey, H. Ågren, P. N. Prasad, G. Han, *ACS Nano* **2012**, *6*, 8280.
- [24] P. S. May, A. Baride, M. Y. Hossan, M. Berry, *Nanoscale* **2018**, *10*, 17212.
- [25] E. I. Madirov, V. A. Konyushkin, A. N. Nakladov, P. P. Fedorov, T. Bergfeldt, D. Busko, I. A. Howard, B. S. Richards, S. V. Kuznetsov, A. Turshatov, *J. Mater. Chem. C* **2021**, *9*, 3493.
- [26] S. V. Kuznetsov, P. P. Fedorov, *Inorg. Mater.* **2008**, *44*, 1434.
- [27] D. Hudry, A. De Backer, R. Popescu, D. Busko, I. A. Howard, S. Bals, Y. Zhang, A. Pedraza-Tardajos, S. Van Aert, D. Gerthsen, T. Altantzis, B. S. Richards, *Small* **2021**, *17*, 2104441.
- [28] Y. Li, Y. Gu, W. Yuan, T. Cao, K. Li, S. Yang, Z. Zhou, F. Li, *ACS Appl. Mater. Interfaces* **2016**, *8*, 19208.
- [29] J. C. de Mello, H. F. Wittmann, R. H. Friend, *Adv. Mater.* **1997**, *9*, 230.
- [30] D. O. Faulkner, J. J. McDowell, A. J. Price, D. D. Perovic, N. P. Kherani, G. A. Ozin, *Laser Photonics Rev.* **2012**, *6*, 802.
- [31] R. E. Joseph, D. Busko, D. Hudry, G. Gao, D. Biner, K. Krämer, A. Turshatov, B. S. Richards, I. A. Howard, *Opt. Mater.* **2018**, *82*, 65.
- [32] P. A. Popov, P. P. Fedorov, V. A. Konyushkin, A. N. Nakladov, S. V. Kuznetsov, V. V. Osiko, T. T. Basiev, *Doklady Phys.* **2008**, *53*, 413.
- [33] X. Zheng, R. K. Kankala, C.-G. Liu, Y. Wen, S.-B. Wang, A.-Z. Chen, Y. Zhang, *Adv. Opt. Mater.* **2022**, *10*, 2200167.
- [34] J. Huang, L. Yan, S. Liu, L. Tao, B. Zhou, *Mater. Horiz.* **2022**, *9*, 1167.
- [35] Y. Shang, Q. Han, S. Hao, T. Chen, Y. Zhu, Z. Wang, C. Yang, *ACS Appl. Mater. Interfaces* **2019**, *11*, 42455.
- [36] B. Zhou, B. Tang, C. Zhang, C. Qin, Z. Gu, Y. Ma, T. Zhai, J. Yao, *Nat. Commun.* **2020**, *11*, 1174.
- [37] B. Chen, Y. Wang, Y. Guo, P. Shi, F. Wang, *ACS Appl. Mater. Interfaces* **2021**, *13*, 2327.
- [38] S. Kedenburg, M. Vieweg, T. Gissibl, H. Giessen, *Opt. Mater. Express* **2012**, *2*, 1588.
- [39] H. H. Li, *J. Phys. Chem. Ref. Data* **1980**, *9*, 161.
- [40] S. Leyre, E. Coutino-Gonzalez, J. J. Joos, J. Ryckaert, Y. Meuret, D. Poelman, P. F. Smet, G. Durinck, J. Hofkens, G. Deconinck, P. Hanselaer, *Rev. Sci. Instrum.* **2014**, *85*, 123115.